APPLICATION OF A SCALAR STRAIN-BASED DAMAGE ONSET THEORY TO THE FAILURE OF A COMPLEX COMPOSITE SPECIMEN

Tuyen Tran*, Dan Simkins, Shen Hin Lim*, Donald Kelly*, Garth Pearce*,**
B. Gangadhara Prusty*, Jon Gosse*, Steve Christensen*****
University of New South Wales, **University of South Florida,
*****The Boeing Company**
g.pearce@unsw.edu.au

Keywords: *Onset Theory, distortional invariant, dilatational invariant, meshfree methods*

Abstract

Application of a scalar strain-based damage onset theory to the failure of a [0_2/90_4/0_2] carbon fibre specimen loaded in tension is described in this paper. A multi-scale modelling process has been utilized to model the cross-ply laminate. Micromechanical sub-models are derived from a laminate shell or layered solid finite element model. These models enable direct de-homogenization of the strain fields. Strain invariants can then used to predict the onset of damage within both fibre and matrix phases. In addition these strain fields allow the type of deformation (dilatation or distortion) to be identified. An explicit crack emergence and growth method is then used to analyse the emerging micro-crack network within the matrix phase of a laminated cross-ply arch.

1 Introduction

Composite materials have been shown to make an important contribution to the development of lighter and stronger aerospace structures. To further the application of these materials, the algorithms used to predict strength and failure need to be based on physically correct theories rather than similitude based methods. By similitude based methods we mean methods that either interpolate configurations between tested configurations or extrapolate a tested configuration to configurations in the neighbourhood of the test configuration. Most of the available similitude based methods are based on stress, strain or strain energy and are applied at the laminate level. The physically correct procedures described in this paper identify failure in the fibre and matrix phases and therefore require de-homogenization of homogenized strain tensors to the fibre and matrix constituent level. They are also well supported by analysis at the molecular level executed using molecular dynamics algorithms.

Recently, Gosse and Christensen [1] and Hart-Smith [2] proposed a micromechanics failure theory for composites, called Strain Invariant Failure Theory (SIFT), or more recently the Onset Theory [3]. This failure theory is based on the use of critical strain invariants to predict the onset of damage. The onset theory is considered to be rigorous and have unique advantages over traditional failure theories in that it is suitable for all possible laminate lay-ups, geometric configurations, loading and boundary conditions. Implementation of the theory involves determining microscopic strains in the polymeric matrix phase, the fibre phase and at the fibre/resin interface of composite laminates. Recent molecular dynamics investigations [4] have injected considerable insight into the physical failure mechanisms and have been used to confirm the critical values of the invariants that have been determined by experimentation on unidirectional test specimens.

Finite element analysis using plate, shell or layered brick elements provides ply strains within the laminate. In the *classical* onset theory

these ply strains are enhanced using influence functionals [3] to determine strains within the matrix and fibre phases. In this paper a novel micromechanical sub-modelling approach will be implemented to de-homogenize the strains. The scalar strain-based damage onset theory is then applied to determine the onset of failure. Damage evolution and cracking is predicted using an explicit crack emergence and growth method based on the Reproducing Kernel Particle Method (RKPM) [5]. In this method, the growth of the damage is assessed using the Onset Theory and is expressed with RKPM.

2 Review of Onset Theory

Onset Theory is based on strain invariants [1, 3, 6-7]. It is a recent development for glassy polymers constrained by fibres in structural composites, although the theory applies to the constrained glassy polymeric adhesives as well Recognizing that the mechanics of the failure of constrained polymers is based on the drawing apart or changes of the conformation of the molecules, two criteria have been developed. The first predicts micro-cracking from dilatation of the polymer and the second predicts irreversible distortional deformation using the square root of the second strain invariant of the strain deviator tensor. These scalar strain invariants are used to define the 'onset' of the irreversible behaviour.

Onset Theory uses engineering strain $\epsilon = \frac{\Delta L}{L}$ and includes the strains due to the temperature changes that occur during the cure. We note however that, for a uniform material, a change of temperature causes a uniform scaling of size that will not cause stresses nor contribute to failure. It is the elastic strains due to the difference between the thermal expansion coefficients of the individual plies in a laminate, or the difference in the thermal expansion coefficients of the fibre and resin that are of concern. We therefore define the elastic strain as the total strain with the thermal expansion removed.

$$\begin{pmatrix} \varepsilon_{E,x} \\ \varepsilon_{E,y} \\ \varepsilon_{E,z} \\ \gamma_{E,xy} \\ \gamma_{E,yz} \\ \gamma_{E,zx} \end{pmatrix} = \begin{pmatrix} \varepsilon_{x} \\ \varepsilon_{y} \\ \varepsilon_{z} \\ \gamma_{xy} \\ \gamma_{yz} \\ \gamma_{zx} \end{pmatrix} - \begin{pmatrix} \alpha\Delta T \\ \alpha\Delta T \\ \alpha\Delta T \\ 0 \\ 0 \\ 0 \end{pmatrix} \quad (1)$$

The distortional and dilatational strain invariants are then derived as shown in Equations 2 and 3.

$$\begin{aligned} \varepsilon_{dilatational} &= \varepsilon_{E,1} + \varepsilon_{E,2} + \varepsilon_{E,3} \\ &= \varepsilon_{E,x} + \varepsilon_{E,y} + \varepsilon_{E,z} \end{aligned} \quad (2)$$

$$\begin{aligned} &\varepsilon_{distortional} \\ &= \sqrt{\frac{1}{6}\begin{bmatrix} \left(\varepsilon_{E,1} - \varepsilon_{E,2}\right)^2 + \left(\varepsilon_{E,2} - \varepsilon_{E,3}\right)^2 \\ +\left(\varepsilon_{E,1} - \varepsilon_{E,3}\right)^2 \end{bmatrix}} \\ &= \sqrt{\frac{1}{6}\begin{bmatrix} \left(\varepsilon_{E,x} - \varepsilon_{E,y}\right)^2 + \left(\varepsilon_{E,y} - \varepsilon_{E,z}\right)^2 \\ +\left(\varepsilon_{E,x} - \varepsilon_{E,z}\right)^2 \end{bmatrix} + \frac{1}{4}\left(\gamma_{E,xy}^2 + \gamma_{E,yz}^2 + \gamma_{E,zx}^2\right)} \end{aligned} \quad (3)$$

$\varepsilon_{dilatational}$ = dilatational strain invariant
$\varepsilon_{distortional}$ = distortional strain invariant
$\varepsilon_{E,1}$, $\varepsilon_{E,2}$, $\varepsilon_{E,3}$= principal elastic strains
$\varepsilon_{E,x}$, $\varepsilon_{E,y}$ and $\varepsilon_{E,z}$= normal elastic strains in the Cartesian coordinate system
$\gamma_{E,xy}$, $\gamma_{E,yz}$ and $\gamma_{E,zx}$ = engineering shear strain components in the Cartesian coordinate system

An important feature of the onset theory is the de-homogenization of homogenous strains in the plies to give strains in the fibre and matrix phases of the composite material system. The micromechanical modelling procedure used in this paper is described the Section 3. Damage onset within the matrix phase is then applied as follows.

Matrix cavitation will occur if

$$\varepsilon_{dilatational} \geq \varepsilon_{dilatational}^{critical} \quad (4)$$

Matrix yielding will occur if

$$\varepsilon_{distortional} \geq \varepsilon_{distortional}^{critical} \quad (5)$$

where the critical values are intrinsic material properties.

3 A micromechanical sub-modelling approach to determine resin and fibre strains from average ply strains

A micromechanical sub-modelling procedure is applied in this paper to determine detailed resin and fibre strains from average ply strains in the laminate.

The first step is to choose a fibre pattern that will be the basis of the sub-model. For the work in this paper the square array in Fig. 1 is used because it has been shown to give conservative local strains in the resin for 90° plies. A three-dimensional sub-model with the correct fibre-volume fraction is then created and embedded in the laminate finite element mesh as shown in Fig. 2.

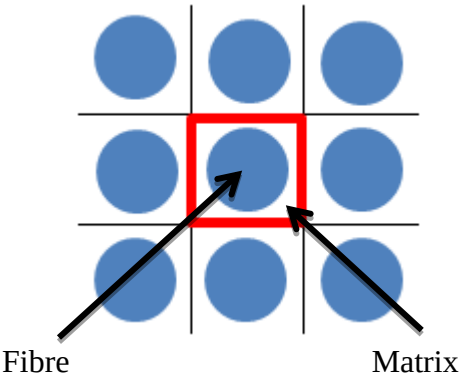

Fig. 1. Representative fibre configuration for a square array of fibres

Displacements calculated on the cut boundary of the global model are transferred to the sub-model as boundary conditions. Plotting the strain invariants in the 3D model allows for a visualization of the micromechanical strain fields for the matrix phase and for the fibre phase. These strain fields allow for a prediction of the onset of damage as well as type of deformation (i.e. distortional or dilatational) using the onset theory.

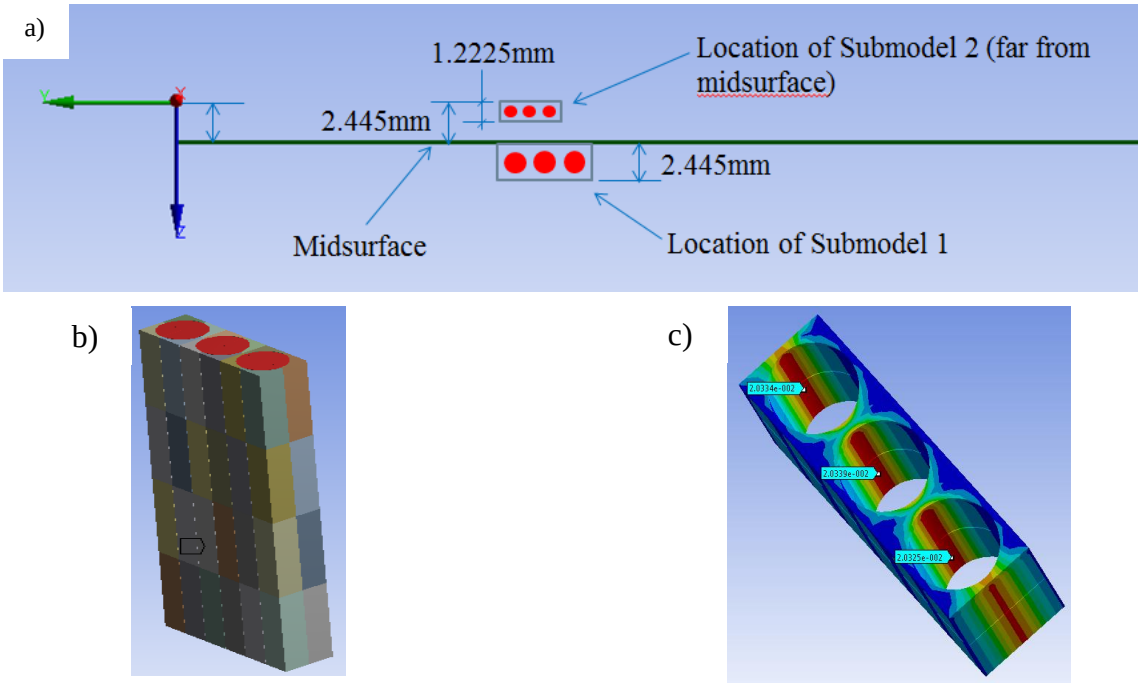

Fig. 2. (a) A plate–shell finite element model and (b) micromechanical sub-model for the 90° off-axis specimen. (c) Plot of the dilatational invariant

The procedure for extracting the strains is as follows:

- Analyse the laminate model with the applied mechanical loads using the sub-model to define the elastic strains ϵ_E^M.
- Analyse the laminate model with free boundaries but $\Delta T = T - T_{cure}$ using the sub-model to define the elastic strain due to thermal effects ϵ_E^T.
- Superimpose elastic strains

$$\varepsilon_i^k = \left(\epsilon_{E,i}^M + \varepsilon_{E,i}^T\right) \qquad (i = 1 - 6)$$

The strains ε_i^k are the micro-elastic strains to insert into Equations 1 and 3 for the strain invariants. These strains automatically include the magnification due to the fibre/matrix interaction.

Composite laminates can be modelled using shell or layered solid or solid continuum elements depending on the geometries, lay-ups and details of results required. Solid-to-solid and shell-to-solid sub-modelling approaches (available in ANSYS Version 12.1) are used in this research. Care must be taken when shell-to-solid sub-modelling is conducted since the approach implemented in this software has some restrictions on the interpolation of the nodal values at the cut boundaries.

Fig. 2 shows a micromechanical sub-model for the shell 90° off-axis continuum analysis. The sub-model includes a single array of fibres. Three-dimensional finite element analysis of the sub-model is implemented using a refined mesh and the full set of anisotropic properties for the fibre. In an extended approach the sub-model fibre diameters are reduced while the fibre volume fraction is maintained to give multiple layers of fibres in the matrix. This allows for investigating the effects of varying the model fibre diameter with respect to the dilatational and distortional invariants. The diameters of the fibre are calculated such that, for this particular case, the volume fraction of fibres is always maintained at 60% as indicated in the manufacture data sheet for the prepreg material for the specimens used in this study.

4 Determination of the critical invariants

The material system used in this study is T800s/3900-2 material (see Table 1). A first step for the application of the onset theory is the determination of the critical invariants from Equations. Unidirectional off-axis specimens were manufactured with fibres aligned at 10^o and 90^o relative to the load direction (0^o direction).The specimens were tested to failure and the average axial global strain at failure recorded. A full length micromechanical model is then created and the average axial strain at failure from the test applied to the specimen (applied displacements). Local maximum strains in the fibre and matrix are then substituted into Equations 4 and 5 to determine the values of the critical strain invariants. For the plots in Fig. 3 the sub-models have been extended to the full specimen size to show the shear bending (axial/shear coupling) in the 10^o specimen.

Table 1. Properties of effective lamina T800s/3900-2, fibre and matrix

Properties	Lamina	T800s Fibre	3900-2 Epoxy resin
E_1 (GPa)	152	303	3.3
E_2 (GPa)	8	15.2	3.3
E_3 (GPa)	8	15.2	3.3
G_{12} (GPa)	4	9.65	1.22
G_{23} (GPa)	2.75	6.32	1.22
G_{13} (GPa)	4	9.65	1.22
ν_{12}	0.34	0.2	0.35
ν_{23}	0.45	0.2	0.35
ν_{13}	0.34	0.2	0.35
$\alpha_{11}(/^0C)$	3.6e-8	0	57.6e-6
$\alpha_{22}= \alpha_{33}$ $(/^0C)$	37.8e-6	8.3e-6	57.6e-6

The extracted critical strain invariants are given in Table 2. The extent of the current study was limited to the matrix phase only. Therefore, only the critical values for the matrix phase are reported here.

Table 2. Critical matrix invariants for T800s/3900-2

Mode	Dilatation	Distortion
Resin	0.0225	0.1170

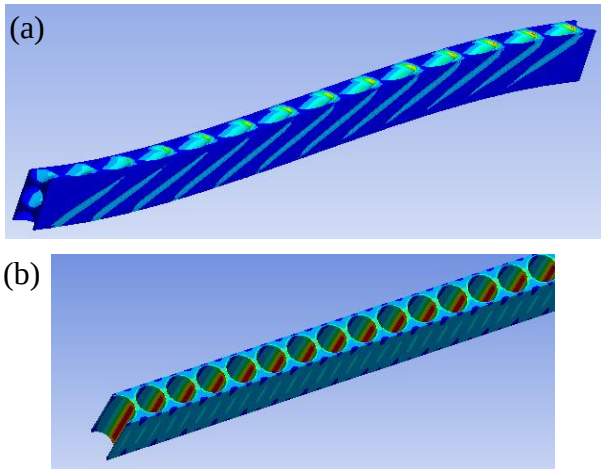

Fig. 3. Micromechanical models used to determine the de-homogenized strains for the (a) 10° and (b) 90° specimens.

Finally we note that the material properties for the laminate in Table 1 cannot be derived from the rule of mixtures using the properties given for the fibre and matrix. The decision in this work was to use the best available transverse properties available for the fibre phase and the laminate. The determination of improved properties is the subject of further experimental investigation.

5 Damage Progression

Although the onset theory introduced above pertains to both the polymeric matrix and fibre phases of composite material systems only the polymeric matrix phase is addressed in this paper. Glassy polymers within composite material systems and adhesive bondlines are constrained. Therefore, not only is critical distortional deformation realized but critical dilatational deformation as well. Both forms of deformation appear to manifest damage initiation as cavitation due to the non-uniform strain distributions between the fibres. As a result, post-yield flow does not occur in these systems (for effective fibre volumes utilized in engineering practice).

After damage initiation, the damage state within constrained glassy polymer systems takes the form of a network of micro-cracks. The authors of this paper utilize convergence to unique limits to define the DOF (degrees of freedom) distribution in their models. This includes damage initiation and damage propagation. With respect to glassy polymer systems this means that all sources of error need to be removed or significantly mitigated in order for convergence to approach the unique limit of the material system. One significant source of error is in the choice of the damage initiation criteria. Crack propagation is really damage initiation over and over again [8]. Therefore, the wrong choice of this major decision maker in the analysis methodology can have profound effects on the outcome of the analysis. For constrained glassy polymer systems only the scalar strain invariants can be used to assess damage initiation (and therefore propagation). All solids have at most two critical properties, the dilatational and distortional strain invariants. Whether these strain invariants are reflected in stress (and therefore strain energy) space depends on whether or not the material system is essentially linear-to-critical (for example, like mild steel) or not. For operating temperatures of most engineered composite structures glassy polymer systems are nonlinear-to-critical due to anelasticity (the reversible part of nonlinear viscoelasticity) [9]. It has been clearly demonstrated that the stresses (and therefore the strain energy densities) are not unique at critical for glassy polymer systems but the scalar strain invariants are [10].

When considering the simulation of cracks one naturally thinks of fracture mechanics. The above argument does not allow any use of stress or energy release to be used in analysis methodology attempting to approach the unique limit of a given glassy polymer system. This fact pertains to both VCCT and cohesive elements as well (stress or force/displacement laws).

The use of finite element methods to model crack networks is addressed nicely by Mohammadi [11]. The use of the finite element method is feasible for this task but has issues that have led to the development of the extended finite element method (X-FEM). For the complex cracking networks that need to be

simulated in composite material systems it would appear that the flexibility that meshfree methods afford is necessary. Although it has been shown within the Boeing Co. that convergence at the free-edges of laminates can be achieved with the scalar strain form of the onset theory, sharp crack tips, sharp corners and strain localization are most effectively addressed (with respect to convergence) with the nonlocal shape functions of meshfree methods (weak form for applied mechanics) [5]. If convergence can be realized then there cannot be any mesh dependency.

In this paper, a bent beam (an arch) consisting of a [0/90/0/90/0] laminate configuration (90^o plies coming out of the board) is modelled subject to opposing horizontal displacements at the base (see Fig. 4). The red plies are the fibres coming out of the page. The grey image is the deformed shape subject to opposing horizontal displacements applied at the base of the structure.

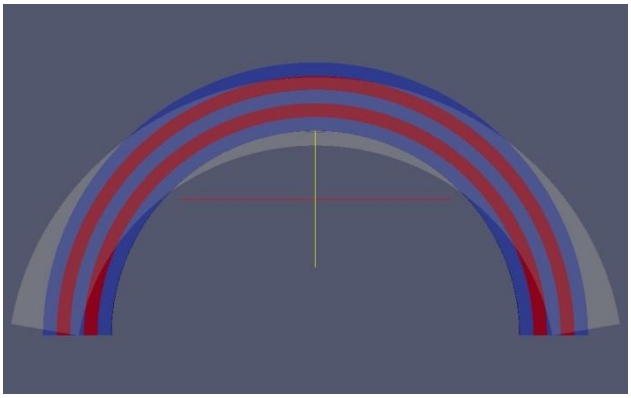

Fig. 4. An arch with a cross-ply laminate configuration [12]

The material properties used in this exercise are similar to those given in Table 1. Both applied mechanical and applied thermal loads are considered resulting in a total strain analysis. The strain-free temperature was 177°C and the test temperature, 25°C. The arch is 3D in that it has a unit dimension into the page. Damage initiation is realized as explained above resulting in split nodes. Shape functions are re-written to reflect the change in topology. Once equilibrium has been realized step loads are applied and a new crack tip is sought and examined for failure by the onset theory. A 2D representation of the process is shown in Fig. 5.

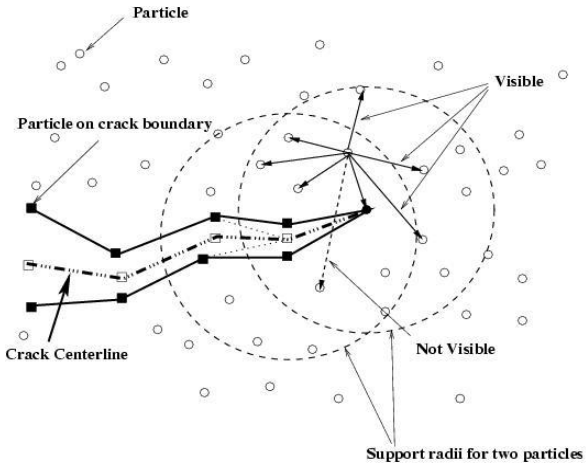

Fig. 5. A 2D representation of the meshfree crack propagation simulation [5, 13]

The present method utilizes an embedded meshfree submodel within a larger finite element model thereby improving computational efficiency and removing the essential boundary issues associated with meshfree methods. Continuous blended elements are used at the interface of the meshfree and finite element domains. This concept is used by both meshfree and X-FEM analysis methodologies [5, 11].

6 Result and Discussion

6.1 Specimen Preparation and Testing

$[0/90_2/0]$ and $[0_2/90_4/0_2]$ specimens were manufactured using T800s/3900-2 materials. These specimens were tested using an MTS model 647 servo-hydraulic mechanical test machine with SurfAlloy grip faces. All testing was performed in stroke control at a rate of 1.4mm per minute. Strain data was recorded with an MTS model 632.17B-20 axial extensometer with 50mm gauge length. Hydraulic grip pressure is adjusted to ensure that the specimens are not crushed but also do not slip due to the loading.

Table 3. Failure stress and strain for the $[0/90_2/0]$ specimens

Test	Failure Strain, ε (mm/mm)	Failure Stress, σ (MPa)	Failure Load (N)
1	0.01768	1478.39	58180
2	0.01785	1496.47	58798
Average	0.01776	1487.43	58489
Max	0.01785	1496.47	58798
Standard deviation (%)	0.47473	0.6078	0.5280

Table 3 shows the failure strain, stress and load for the $[0/90_2/0]$ specimens while Fig. 6 shows two typical load-deflection curves.

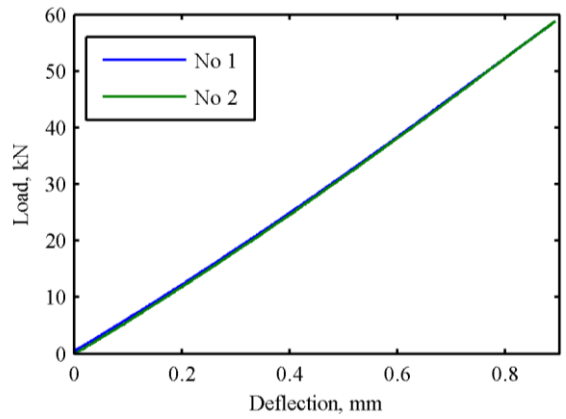

Fig. 6. Load deflection curve for $[0/90_2/0]$

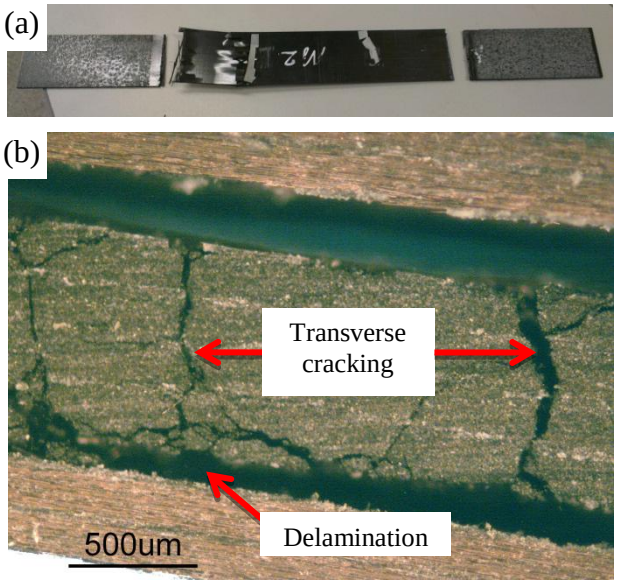

Fig. 7. Images of the failed specimens (a) fracture locations and (b) damage modes

Fig. 7 shows images of the failure specimens. Delamination between 0° and 90° plies is apparent in this case. Testing to failure of the specimens was limited to the $[0/90_2/0]$ configuration since the failure load of the $[0_2/90_4/0_2]$ specimens was predicted to exceed the 100kN load capacity of MTS machine. During the tests of both the $[0/90_2/0]$ and the $[0_2/90_4/0_2]$ specimens multiple cracks found in the 90^o plies at an axial strain in the specimen of approximately 0.004.

6.1 Micromechanical Analysis for Damage Onset

Only the test section of the specimen is modelled. The specimen was analysed using layered brick elements in the ANSYS system and a submodel was created to provide the de-homogenised fibre and matrix strains. The models used are shown in Fig. 8. All nodes at the left end face are constrained with $u_x=u_y=u_z=0$ while those at the right end face are constrained with $u_y=u_z=0$ and $u_x=\varepsilon L$. Since the analysis is elastic, a single analysis was used to define the average specimen axial strain for which the dilatational invariant was equal to the critical value. This occurred for an average axial strain of 0.0046.

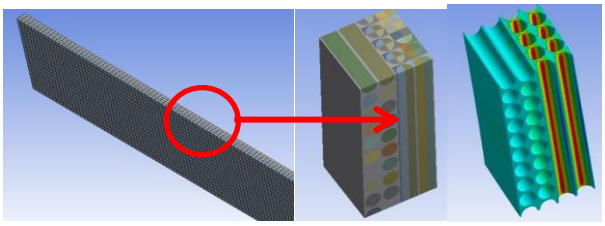

Fig. 8. Analysis for initial cracking in the 90° plies

6.2 Crack emergence and crack growth results

The initial damage within the loaded arch is a dilatational failure between the bottom ply (0° ply) and the next ply up (90° ply). The region of interest is shown in Fig. 9 (the yellow circle). This is where damage will initiate.

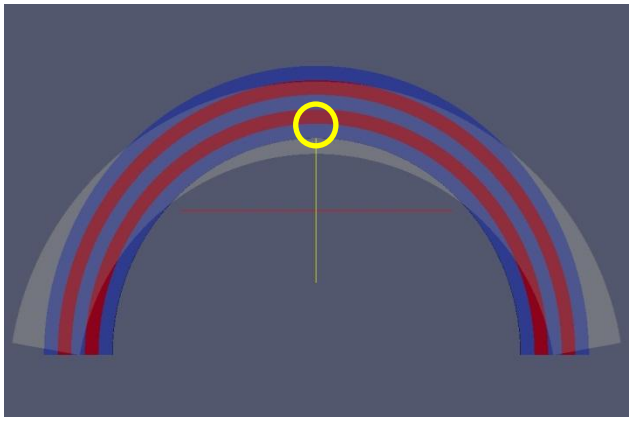

Fig. 9. Region of interest

The most active strain invariant in this problem is the dilatational strain invariant. The red regions in Fig. 10 illustrate the regions of high dilatational strain invariant just prior to damage initiation.

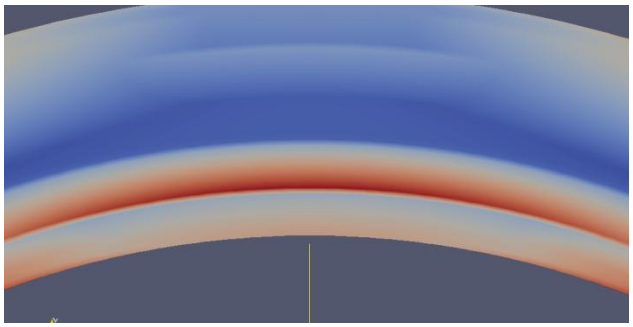

Fig. 10. Distribution of the dilatational strain invariant just prior to damage initiation [12]

Damage initiates between the plies and is therefore a delamination (see Fig. 11).

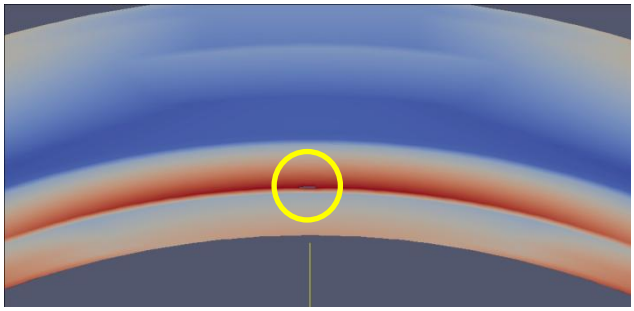

Fig. 11. Region of delamination initiation

The delamination propagates without initiating transverse cracks along the 0/90 interface (see Fig. 12).

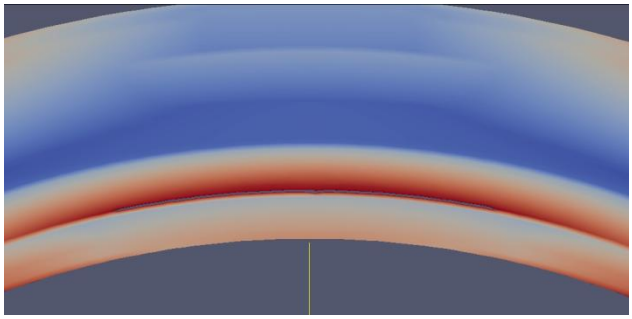

Fig. 12. Delamination propagation

At some point a transverse crack is initiated within the second ply (90^o ply). The transverse crack is initiated by the critical dilatational invariant, see Fig. 13.

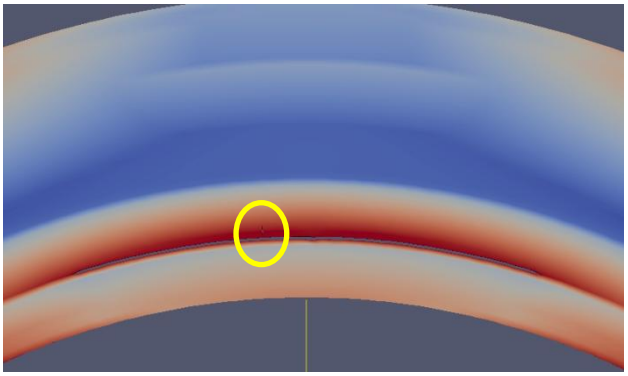

Fig. 13. Initiation of a single transverse crack

Continued propagation reveals several transverse cracks within the second ply (see Fig. 14).

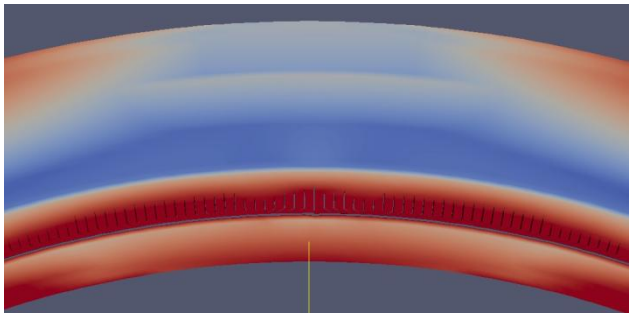

Fig. 14. A single delamination between plies 1 and 2 and several transverse cracks within ply 2 [12]

The simulated sequence of events was later validated by comparison with test data of similar configuration used to support Boeing products. The simulation could have been

continued resulting simulated fibre failures as well.

It should be noted that at no time was a starter crack inserted into this simulation and only the true critical properties of the glassy polymers were used to simulate the state of damage as a function of loading.

7 Conclusion

This paper has focused on presenting an application of a scalar strain-based damage onset theory to the failure of the matrix phase of a complex composite specimen. It has presented a new sub-modelling approach for implementing the analysis required to determine the explicit assessment of the strains within the matrix and fibre phases. Damage initiation is verified using the onset theory and a qualitative assessment of damage initiation and subsequent propagation (continued initiation) presented.

References

1. Gosse, J.H. and S. Christensen, Strain Invariant Failure Criteria for Polymers in Composites, in 42nd AIAA Structures, Structural Dynamics and Materials Conference and Exhibit. 2001: Seattle, USA. p. 45-55.

2. Hart-Smith, L.J., Mechanistic Failure Criteria for Carbon and Glass Fibers Embedded in Polymers in Polymer Matrices, in 42nd AIAA Structures, Structural Dynamics and Materials Conference and Exhibit. 2001: Seattle, USA.

3. Pipes, R.B. and J.H. Gosse, An Onset Theory for Irreversible Deformation in Composite Materials, in 17th International Conference on Composite Materials (ICCM-17). 2009: Edinburgh, UK.

4. Christensen, S., Onset Theory Informed Virtual Formulation of a New Composite Matrix using Molecular Dynamics with Selected Experimental Validation, in International Conference on the Mechanics of Nano, Micro and Macro Composite Structures (ICNMMCS), A.J.M. Ferreira and E. Carrera, Editors. 2012: Torino, Italy.

5. Li, S. and W.K. Liu, Meshfree Particle Methods. 2007: Springer.

6. Buchanan, D.L., et al., Micromechanical Enhancement of the Macroscopic Strain State for Advanced Composite Materials. Composites Science and Technology, 2009. 69(11-12): p. 1974-1978.

7. Tran, T.D., et al., Micromechanical Modelling for Onset of Distortional Matrix Damage of Fiber Reinforced Composite Materials. Composite Structures, 2012. 94(2): p. 745-757.

8. Anderson, T.L., Fracture Mechanics: Fundamentals and Applications. 1995: CRC Press.

9. Caruthers, J.M., et al., A Thermodynamically Consistent, Nonlinear Viscoelastic Approach for modeling Glassy Polymers. Polymer, 2004. 45(13): p. 4577-4597.

10. Capaldi, F.M., M.C. Boyce, and G.C. Rutledge, Molecular response of a glassy polymer to active deformation. Polymer, 2004. 45(4): p. 1391-1399.

11. Mohammadi, S., Extended Finite Element Method: for Fracture Analysis of Structures. 2008: Blackwell Publishing.

12. Simkins, D.C., Multi-scale Structural Mechanics for Advanced Aircraft Design. Journal of Nonlinear Systems and Applications, 2012. 3(1): p. 41-45.

13. Simkins, D.C. and S. Li, Meshfree simulations of thermo-mechanical ductile fracture. Computational Mechanics, 2006. 38(3): p. 235-249.

Acknowledgement

This research has been supported by the ARC Linkage Project LP100200607.

Copyright Statement